ELSEVIER

Journal of Chromatography A, 944 (2002) 225–240

JOURNAL OF CHROMATOGRAPHY A

www.elsevier.com/locate/chroma

Separation of binaphthol enantiomers through achiral chromatography

Renato Baciocchi[a], Gianmarco Zenoni[b], Marco Mazzotti[c], Massimo Morbidelli[b,*]

[a]*Università di Roma "Tor Vergata", Dipartimento di Scienze e Tecnologie Chimiche, via della Ricerca Scientifica 1, I-00133 Rome, Italy*

[b]*ETH Zürich, Laboratorium für Technische Chemie, LTC, CAB C40 Universitätstrasse 6, CH-8092 Zurich, Switzerland*

[c]*ETH Zürich, Institut für Verfahrenstechnik, CH-8092 Zurich, Switzerland*

Abstract

Chromatography is a key technique for the analytical, preparative, and production scale separation of enantiomers, particularly in the pharmaceutical and fine chemicals industries. Although it is common belief that this separation can be accomplished only using a chiral stationary phase, it has been recently shown that under certain circumstances a non-racemic mixture of specific chiral compounds can be separated in two fractions which differ in enantiomeric excess (e.e.) also on an achiral stationary phase. In this work we show that in the case of the enantiomers of binaphthol in chloroform achiral chromatography on LiChrospher 100 NH_2 furnishes two fractions constituted of the pure enantiomer present in excess and of the racemic mixture, respectively. This is demonstrated by on-line monitoring the concentration of both enantiomers at the outlet of a chromatographic column fed with a non-racemic pulse of the two enantiomers by using a UV detector and a polarimeter in series. Furthermore, we provide experimental evidence of the presence of homo- and hetero-dimers in solution through NMR experiments and develop a consistent physico-chemical model of the solution itself and of the competitive achiral adsorption equilibria. When combined with a standard rate model of the chromatographic column this not only confirms the possibility of achieving 100% e.e. through achiral chromatography, but also allows for a qualitative and quantitative description of all the experimentally observed phenomena. Among these, the effect of the enantiomeric excess and of the overall concentration of the injected pulse on the chromatographic behaviour are worth mentioning.

Keywords: Enantiomer separation; Mathematical modelling; Adsorption isotherms; Binaphthol

1. Introduction

Adsorption-based separations and chromatographic methods play a key role in the bulk separation and purification of high-value species, such as pharmaceutical active substances and products obtained through bio-technological routes. In particular, pure enantiomers of chiral compounds can be obtained via either chromatographic separation of racemates produced through symmetric synthesis or chromatographic purification of the products of enantioselective synthesis (either chemical or enzymatic). In the former case, chiral stationary phases are used, which are nowadays stable enough to allow for preparative and industrial scale separation of enantiomers, particularly using the simulated moving bed technology [1].

Although it is generally taken for granted that a

*Corresponding author. Tel.: +41-1-632-3034; fax: +41-1-632-1082.

E-mail address: morbidelli@tech.chem.ethz.ch (M. Morbidelli).

0021-9673/02/$ – see front matter
PII: S0021-9673(01)01366-8

chiral selector is needed to achieve enantioseparation, in the case of a non-racemic feed this has also been attained through chromatography on an achiral stationary phase. The pulse injected into the column splits into two fractions, constituted of the excess enantiomer at an e.e. (enantiomeric excess) significantly larger than that of the feed, and of a nearly racemic mixture, respectively. Cundy and Crooks were the first to discover this phenomenon in the case of the enantiomers of nicotine [2]. Similar results were then reported by Charles and Gil-Av for three different α-amino acid derivatives (a diamide, the *N*-trifluoroacetylvaline-valine cyclohexyl ester, and the *N*-trifluoroacetylvalanine-glycine isopropyl ester) [3], by Tsai et al. for a diketone [4], by Dobashi et al. for the *N*-acetylvaline *tert*.-butyl ester [5], by Matusch and Coors in the case of five different compounds (1,1-bi-2-naphthol, 1-anthryl-2,2,2-trifluoroethanol, *N*-benzoylalanine methyl ester, chloromezanone, and camazepam) [6], by Diter et al. for several sulfoxides on silica gel [7], and by Stephani and Cesare in the case of five different antihistamines [8]. The enantiomers of 1,1′-bi-2-naphthol, which is studied in this work and referred to as binaphthol in the following, were separated not only by Matusch and Coors on a LiChrosorb-amine column in hexane–isopropanol (60:40) [6], but also more recently by Nicoud et al. on a LichroCART (NH_2) column in four different solvents, namely pure chloroform, pure dichloromethane and hexane–isopropanol (60:40) and (80:20) [9]. It is worth noting that in none of these works a pure enantiomeric fraction (100% e.e.) has been obtained.

There is agreement in attributing the phenomenon of the enantiomeric enrichment of non-racemic mixtures by achiral chromatography to some sort of non-ideal thermodynamic behaviour of the two enantiomers in the liquid or in the adsorbed phase due to Van der Waals forces or to chemical association, i.e. dimerization. It can be shown that each of these effects can lead to at least partial enrichment of the excess enantiomer, as observed in the experiments. In particular, dimerization has been demonstrated in the case of binaphthol in chloroform [9,10], and it has been accounted for as the controlling mechanism in the models developed by various authors [9,11,12]. To be more specific, in the case of the two enantiomers (**R** and **S**) the dimerization reactions take place according to the following scheme, thus leading to both the homochiral dimers (**RR** and **SS**) as well as the heterochiral dimer (**RS**):

$$\mathbf{R} + \mathbf{R} \rightleftharpoons \mathbf{RR} \quad (1)$$

$$\mathbf{S} + \mathbf{S} \rightleftharpoons \mathbf{SS} \quad (2)$$

$$\mathbf{R} + \mathbf{S} \rightleftharpoons \mathbf{RS} \quad (3)$$

The goal of this work is twofold. On the one hand we investigate again the separation of the enantiomers of binaphthol in chloroform on a LiChrospher 100 NH_2 column. Using an on-line monitoring technique the possibility of achieving 100% e.e. is demonstrated. On the other hand, based on the theoretical understanding of the phenomena involved, a mathematical model of the system is developed. The adsorption isotherm parameters are estimated through properly designed chromatographic experiments, whereas the dimerization equilibrium constant is measured independently following the approach presented recently [10]. The agreement between experimental results and model predictions is verified and discussed.

2. Background

2.1. Modelling

The aim of this section is to review the modelling attempts that have been reported in the literature as briefly mentioned in the Introduction. We will focus on a few contributions where the enantiomeric enrichment achieved through achiral chromatography has been modelled quantitatively, while recognizing that the controlling mechanism is indeed dimerization.

Jung and Schurig have developed the first, rather flexible model of this kind [11], which has been further specialized later [13]. Their assumptions are that the dimerization reactions (1), (2), and (3) take place both in the fluid and in the adsorbed phase. These are equilibrium limited reactions with finite, though fast, reaction rate. Due to symmetry, the equilibrium and rate constants of the first two reactions yielding the homochiral dimers are the same, whereas those of the third reaction are in

principle different. All monomeric and dimeric species are adsorbed; their adsorption isotherm is linear. Due to symmetry, only three different distribution coefficients are needed, namely one for the two enantiomers, another one for the two homochiral dimers, and the last one for the heterochiral dimer. For the sake of consistency, the chemical and phase equilibrium constants must obey a few thermodynamic constraints. Finally, a standard rate model is used to describe column dynamics, and pulse chromatograms. The authors are able to show that different combinations of parameters yield rather different scenarios, which exhibit different elution sequences and are qualitatively similar to what is observed experimentally. However, the need for too many parameters, which are difficult to measure, has prevented the use of the model to simulate directly the experimental data.

In an attempt to keep the model simple enough to allow for explicit mathematical derivations, Kurganov has significantly simplified the physical picture presented above [12]. The key assumptions are that homochiral dimerization (heterochiral dimerization is not considered) and adsorption (linear) are at equilibrium. The main objective is to show that even with linear adsorption isotherms, rather complex chromatograms can be obtained. However, there is no comparison with experimental results, and the model seems too simple to be realistic.

Nicoud et al. have studied both experimentally and theoretically the same separation considered in this work [9]. They show enantiomeric enrichment of non-racemic mixtures, even though 100% e.e. has not been achieved in any of the four solvent systems considered (chloroform, dichloromethane, and hexane–isopropanol, 80:20, and 60:40). Moreover, this behaviour is attributed to fluid phase dimerization, and in chloroform this is proved through ^{1}H-NMR spectra of both pure enantiomers and racemates. Also their model represents a simplification of the more general model proposed by Jung and Schurig. Dimerization can occur only in the fluid phase; this, as well as adsorption of the five monomeric and dimeric species, is assumed to be at equilibrium. Chiral discrimination is the result of the combination of two effects, namely difference in the equilibrium constants of homochiral and heterochiral dimerization and difference in the adsorptivity of homochiral and heterochiral dimers. Column dynamics is simulated using a standard stage model. However, the authors did not try to estimate the individual phase distribution functions or the equilibrium constants only by chromatographic methods, and introduced instead a hybrid model where the effects of dimerization and adsorption of a single enantiomer and the corresponding homochiral dimer are lumped in a single empirical nonlinear isotherm. This can be determined through single enantiomer chromatograms. Injections of racemic and non-racemic mixtures allow determining the effect of heterochiral dimerization and adsorption of the heterochiral dimer. The overall number of parameters in the model is five. The agreement between experimental data and simulation results is acceptable.

2.2. Dimerization

Recently, a general method to evaluate the extent of dimerization of two enantiomers in solution has been proposed and applied to the same system studied in this work [10]. Evidence of dimerization has been provided through NMR diffusion measurements, as well by analysing the nonlinear behaviour of optical rotation and UV absorbance as functions of the difference in the nominal concentration of the two enantiomers. In this way, it was possible on the one hand to estimate the dimerization equilibrium constant and on the other hand to account for dimerization when interpreting optical rotation and UV absorbance measurements. In the case of the enantiomers of binaphthol in chloroform, the dimerization equilibrium constant has been preliminarily estimated as $K = 2.4$ l/mol at 24°C, i.e. at the same temperature of the experiments reported here. Let us now consider the use of a polarimeter and a UV detector to determine the concentrations of the two enantiomers in solution, which in the following are indicated as r and s for **R** and **S**, respectively. The polarimeter and UV signals can be easily combined when no dimerization occurs, to give the desired concentration values [14]. In the presence of dimerization the following equations must be used:

$$m = \frac{-M + \sqrt{M^2 + 4KDA}}{2KD} \tag{4}$$

$$r + s = m(1 + 2Km) \tag{5}$$

$$\frac{r}{s} = \frac{\mu m + \delta K m^2 + P}{\mu m + \delta K m^2 - P} \quad (6)$$

where A is the UV absorbance, and P is the polarimeter signal, both given in V. The coefficients μ and δ for the polarimeter, and M and D for the UV detector are obtained from calibration; the dimerization equilibrium constant K must be estimated beforehand using the method mentioned above [10]. Obtaining r and s from Eqs. (5) and (6) is straightforward.

3. Experimental

3.1. Materials

The 1,1′-bi-2-naphthol molecule was selected as experimental system to be investigated since its enantiomeric enrichment with achiral chromatography was already assessed in the literature [6,9]. The enantiomerism of 1,1′-bi-2-naphthol is that typical of all biphenyls and binaphthyls (such as 1,1′-binaphthyl) and is generally called atropisomerism, i.e. a type of conformational isomerism in which the conformational isomers may be isolated. Namely, the binaphthol molecule has a chiral axis whose helical sense is maintained through hindered rotation about its single bond between the naphthyl groups, the hindering being due to steric congestion. The planar conformation is an energy maximum and the two non-planar axially chiral enantiomers are energy minima, which exist and can be isolated, their interconversion rate being rather low [15].

Enantiomers of 1,1′-bi-2-naphthol were purchased from Fluka (Buchs, Switzerland). Purities of *R*-(+)-1,1′-bi-2-naphthol and *S*-(−)-1,1′-bi-2-naphthol were 99.8% and 99.9%, respectively. Chloroform (99.8% purity) and methanol (99.8% purity) were purchased from J.T. Baker (Deventer, Netherlands); acetonitryl (99.8% purity) was purchased from Fluka.

3.2. Methods

Achiral chromatography of 1,1′-bi-2-naphthol was carried out on a LichroCART column (25 × 0.4 cm I.D, LiChrospher 100 NH_2, 5 μm) purchased from Merck (Darmstadt, Germany). On-line analysis was performed under isocratic conditions on an HP 1100 liquid chromatograph (Hewlett-Packard, Palo Alto, CA, USA) equipped with a quaternary pump, an autosampler and a thermostatted column compartment kept at a temperature of 24°C, and controlled by an HP Chemstation software (Hewlett-Packard). The flow-rate was kept constant and equal to 1 ml/min. The chromatograph was connected in series with: a HP G1315A photodiode array detector (Hewlett-Packard), with selected wavelengths equal to 242 and 305 nm, the former being used for pulse experiments at less than 4–5 g/l concentration and the latter for pulse experiments up to 10 g/l concentration; a UV detector Jasco UV-970 (Jasco International, Tokyo, Japan) provided with a preparative cell, with selected wavelength equal to 308 nm, used for pulse experiments at concentration larger than 10 g/l; a polarimeter Jasco OR-990 (Jasco International), whose detection limit allowed to determine the enantiomeric enrichment for pulse experiments at concentrations larger than 10 g/l. Data from the Jasco equipments were collected through a computer data acquisition system and elaborated using a Labview program. After calibration of these two detectors, and careful measurement of the dead volume between the two analytical cells (required in order to synchronize the two signals), it was possible to measure on-line the concentration of the two enantiomers. Eqs. (4)–(6) were used, with the calibration constants $\mu = 29.2$ V l/mol, $\delta = -60.2$ V l/mol, $M = 17.2$ V l/mol, and $D = 15.1$ V l/mol [10].

Off-line analysis was carried out on a Chiral NEA column (25 × 0.46 cm I.D., Spherical 5 μm, 30 nm average pore size) purchased from YMC (Kyoto, Japan) using a mixture of 90% acetonitrile and 10% methanol as mobile phase. Samples of eluate from the achiral columns, collected at discrete time intervals, were analyzed on the same HPLC system described above. After calibration of the detectors, the concentration of each enantiomer was measured and compared with the on-line analysis results.

4. Results

4.1. Single enantiomer

Pulse experiments with solutions of the single

R-(+)-1,1′-bi-2-naphthol enantiomer, using chloroform as a solvent, were performed on the achiral column. Different solute concentrations, ranging from 0.01 g/l to 30 g/l, and different pulse volumes, ranging from 5 to 100 μl, were used. This implies injections ranging from 0.05 to 3000 μg of solute, which allowed investigating from dilute, linear conditions, to overloaded, nonlinear ones. A typical nonlinear chromatogram corresponding to a 10 μg injection is reported in Fig. 1. This exhibits a nonlinear, favourable behaviour, with a sharp adsorption front due to the high efficiency of the column. It is worth noting that the **S** enantiomer behaves exactly in the same way, as expected on such an achiral column.

The variation of the measured peak retention time as a function of the injected amount is illustrated in Fig. 2, and the low range behaviour is evidenced in the insert. As expected in the case of a favourable adsorption isotherm, the peak retention times decrease with the injected amount. What is observed is far from a simple Langmuirian behaviour, and the large curvature of the diagram at low injected amounts seems to indicate energetic heterogeneity of the adsorbent surface.

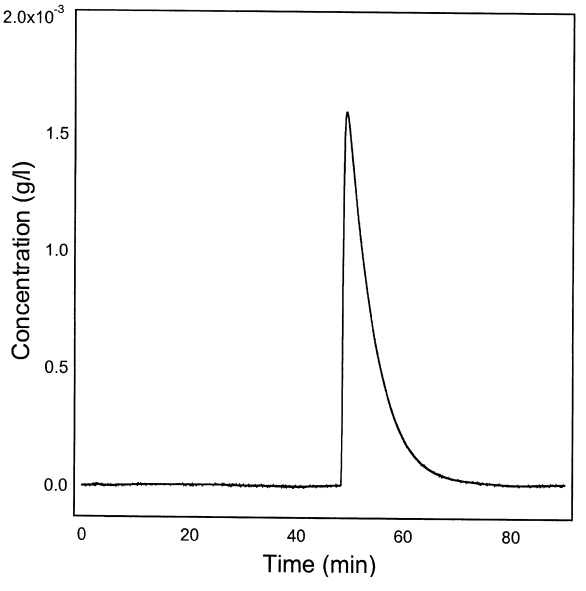

Fig. 1. Elution of a 20 μl pulse of a 1 g/l solution of *R*(+)-1-1′-bi-2-naphthol: concentration profile obtained through UV measurements.

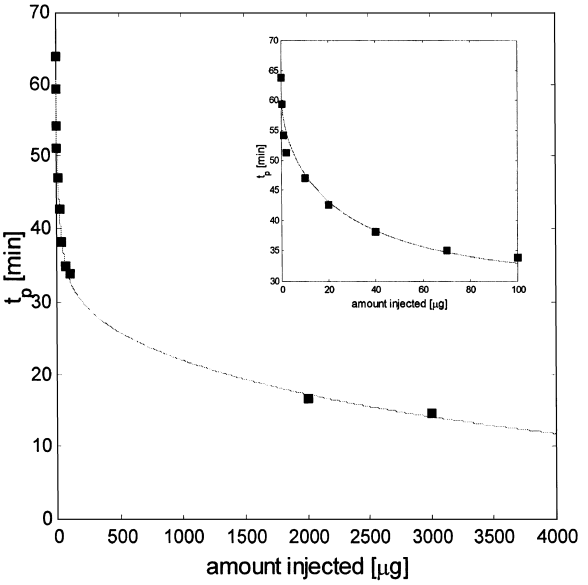

Fig. 2. Experimental (■) and calculated (—) retention times of the peak maximum for pulses of pure *R*-(+)-1-1′-bi-2-naphthol at increasing injected amounts. Insert: zoom on data corresponding to small injected amounts.

4.2. Mixtures of enantiomers

Pulse experiments with mixtures of the two binaphthol enantiomers in chloroform were performed on the same achiral chromatographic column as above. When feeding non-racemic pulses a peculiar behaviour was observed already at low amounts injected, where only the UV detector could be used for monitoring the outlet concentration profile. This does not distinguish between the two enantiomers, hence provides information about the sum of the concentration of the two enantiomers. The result is illustrated in Fig. 3, where a 40 μg pulse, constituted of 80% **S** and 20% **R** enantiomer, splits into two peaks whose retention times differ by about 3 min.

In order to determine the composition of the two peaks, larger amounts were injected and the signals of the UV detector and of the polarimeter were monitored, and combined. The results for a 3000 μg pulse experiment of the same 80:20 mixture are reported in Fig. 4. The UV signal is similar to the one in Fig. 3. The optical rotation measured by the polarimeter and illustrated in the insert of Fig. 4 indicates that the first fraction eluting between about 15 min and about 20 min has a significantly higher

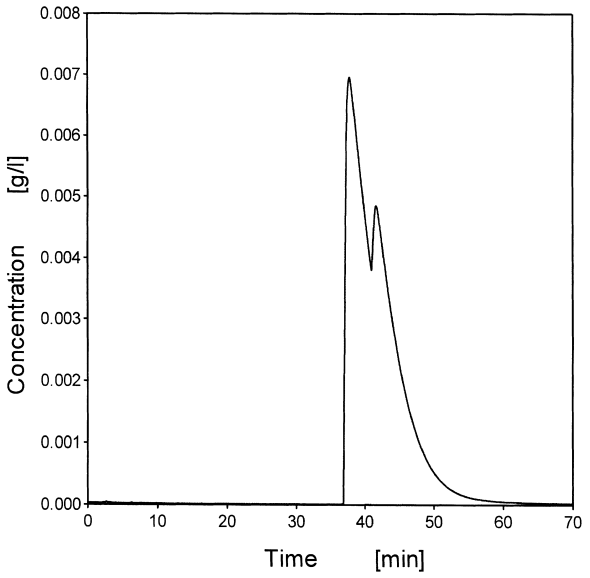

Fig. 3. Elution of a 20 μl pulse of a 2 g/l 80:20 solution of *S*(−) and *R*(+)-1-1′-bi-2-naphthol: concentration profile (sum of the concentrations of the two enantiomers) obtained through UV measurements.

enantiomeric purity than the following fraction. At the time when the second peak breaks through the optical rotation decreases abruptly to a very low value and then decays slowly to zero, i.e. indicating an asymptotic attainment of an equimolar composition of the two enantiomers. These qualitative observations can be quantified by combining the information about UV absorbance and optical rotation using Eqs. (4)–(6), thus obtaining the outlet enantiomer concentrations *r* and *s*. These are plotted in Fig. 5, where some experimental noise can be observed, particularly during the elution of the first **S**-rich peak. Thus, these results were cross-checked by carrying out off-line analysis of a large number of eluate samples collected during the entire pulse experiment at a rate of five samples per minute; each sample was analyzed through chiral HPLC. The results are reported in Fig. 6, and they are practically identical to the on-line concentration profiles of Fig. 5, but for the experimental noise between 15 and 20 min, which does not appear any more. Off-line analysis shows clearly that the first eluting **S**-rich peak is actually a fraction containing only the **S** enantiomer, i.e. exhibiting a 100% e.e. The **R**

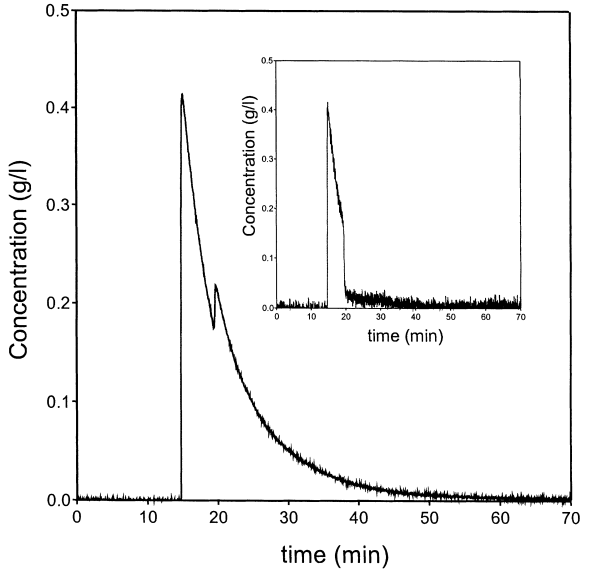

Fig. 4. Elution of a 100 μl pulse of a 30 g/l 80:20 solution of *S*(−) and *R*(+)-1-1′-bi-2-naphthol: concentration profile (sum of the concentrations of the two enantiomers) obtained through UV measurements. Insert: difference between the concentrations of the two enantiomers obtained through optical rotation measurements.

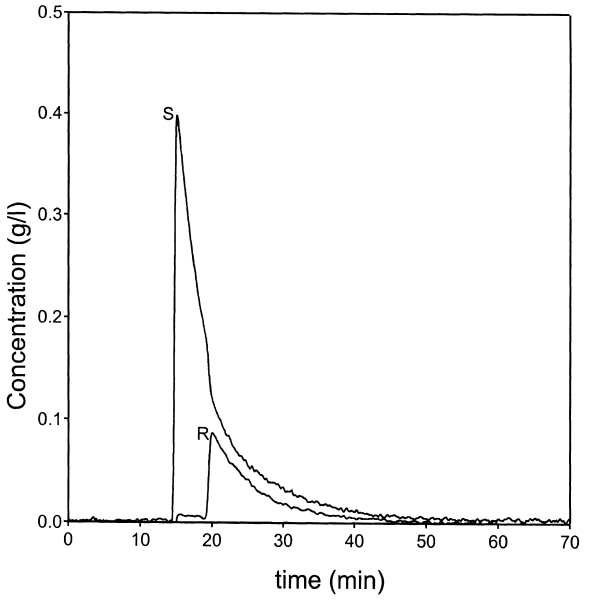

Fig. 5. Elution of a 100 μl pulse of a 30 g/l 80:20 solution of *S*(−) and *R*(+)-1-1′-bi-2-naphthol: concentration profiles of the two enantiomers obtained by combining the on-line UV and polarimeter measurements shown in Fig. 4.

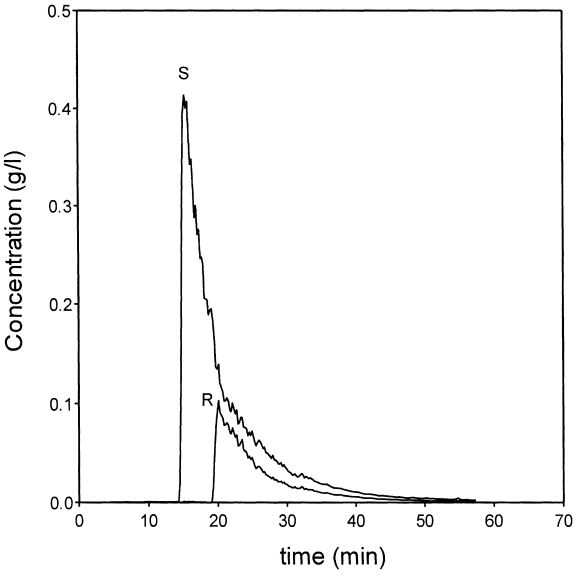

Fig. 6. Elution of a 100 μl pulse of a 30 g/l 80:20 solution of *S*(−) and *R*(+)-1-1′-bi-2-naphthol: concentration profiles of the two enantiomers obtained through off-line chiral chromatography of samples collected periodically at a rate of five samples per minute.

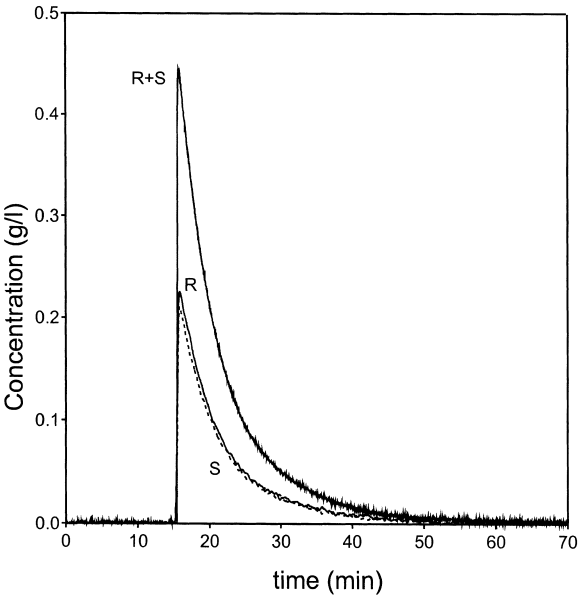

Fig. 7. Elution of a 100 μl pulse of a 30 g/l racemic solution of *S*(−) and *R*(+)-1-1′-bi-2-naphthol: concentration profiles of the two enantiomers obtained by combining on-line UV and polarimeter measurements.

enantiomer breaks through only about 5 min after the **S** enantiomer; the second fraction contains therefore both enantiomers, with a slight excess of the **S** enantiomer and an asymptotic approach to the racemic composition. This proves that 100% e.e. can be achieved through achiral chromatography of a non-racemic mixture. It is worth noting that more than 50% of the enantiomer present in excess in the injected pulse could be recovered in an optically pure fraction. This indicates that the observed phenomenon might be relevant also for preparative purposes.

Apart from this anomalous enantiomeric enrichment, the system behaves in a symmetric way on the achiral column. This is illustrated in Figs. 7 to 10 that elucidate the chromatographic behaviour of pulses with different feed ratios of the two enantiomers. When a racemic pulse is injected there is no enantiomeric enrichment, as illustrated in Fig. 7. The two enantiomers break through at the same time and their concentration profiles clearly overlap, thus maintaining a racemic composition everywhere and at any time along the column. When a 3000 μg pulse constituted of 80% **R** and 20% **S** enantiomer is injected, the symmetric behaviour with respect to

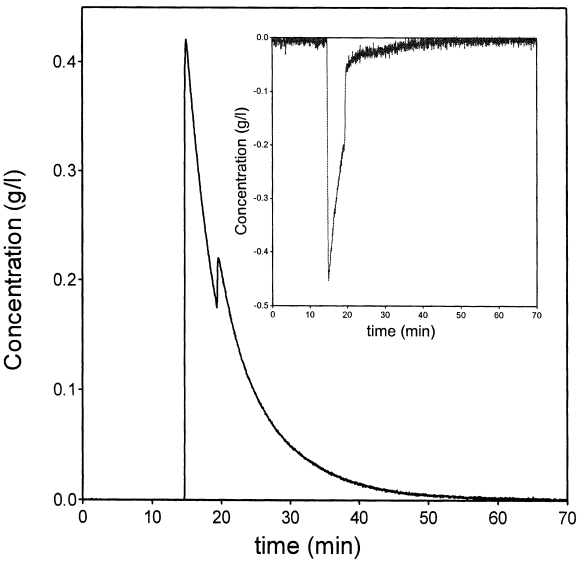

Fig. 8. Elution of a 100 μl pulse of a 30 g/l 20:80 solution of *S*(−) and *R*(+)-1-1′-bi-2-naphthol: concentration profile (sum of the concentrations of the two enantiomers) obtained through UV measurements. In the insert: difference between the concentrations of the two enantiomers obtained through optical rotation measurements.

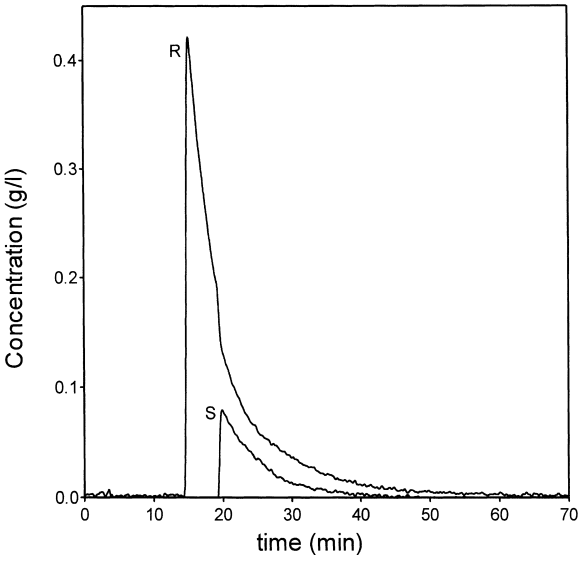

Fig. 9. Elution of a 100 μl pulse of a 30 g/l 20:80 solution of *S*(−) and *R*(+)-1-1′-bi-2-naphthol: concentration profiles of the two enantiomers obtained by combining the on-line UV and polarimeter measurements shown in Fig. 8.

that shown in Fig. 4 is observed. As shown in Fig. 8, the same UV absorbance profile is obtained, whereas the optical rotation profile in the insert is just the opposite of the one reported in Fig. 4 for the 80:20 **S**/**R** mixture. This is further confirmed when combining the polarimeter and the UV signals to obtain the outlet concentration profiles of each enantiomer reported in Fig. 9. Also in this case, a large percentage of the excess **R** enantiomer can be recovered in an optically pure fraction which elutes before a second fraction where the concentrations of the two enantiomers are similar, with a slight, slowly decaying excess of the **R** enantiomer itself.

The same pattern of behaviour exhibited by the experiments in Figs. 6 and 9 was observed in a fairly large number of experiments that were carried out by injecting different amounts of non racemic mixtures with different relative compositions of the two enantiomers and that we do not report here for the sake of brevity. In all cases where a non-racemic mixture was injected, the pulse split in a first fraction constituted of the excess enantiomer eluted first at 100% e.e. and in a second fraction with an e.e. slightly different from zero. Enantiomers injected as a racemate broke through always together, exhibiting no enrichment.

The effect of feed composition on the resolution of the two peaks is measured by injecting the same overall amount of the two enantiomers but with different relative compositions. The results for 3000 μg and 2000 μg injected are illustrated in Fig. 10(a) and (b), respectively. In the diagrams the retention time of the peaks of the two enantiomers is plotted as a function of the feed composition, expressed in percentage of the **S** enantiomer. From the results presented in Figs. 5 and 9 it is clear that the smaller retention time corresponds to the excess enantiomer, whereas the larger time refers to the other; it is also clear that the experimental measurement of the peak retention times is rather easy due to the sharpness of the peaks themselves. As expected, the diagrams are symmetric with respect to the 50% vertical axis. Retention times are the same for a racemic pulse, and exhibit larger and larger differences for concentration of one of the two enantiomers increasing from 50 to 100%. Moreover, the breakthrough time of the excess enantiomer increases slightly when changing the relative composition from pure enantiomer to racemic mixture. As already observed previously [6], the racemate pulse is reproducibly retarded by slightly more than 1 min with respect to single enantiomer pulses of the same overall concentration.

5. Modelling

In the following, we develop a mathematical model accounting for dimerization, adsorption, and column dynamics, to describe chromatograms such as those presented above.

5.1. Dimerization and adsorption

The following assumptions about the phase equilibria and the chemical reactions involved in the system under examination are made. First, the **R** and **S** enantiomers partially dimerize according to reactions (1)–(3), yielding two enantiomeric homochiral dimers, i.e. **RR** and **SS**, and a heterochiral dimer, i.e. **RS**, which is a diastereomer of the two homochiral dimers. Secondly, the three reactions take place only in the fluid phase, and are at

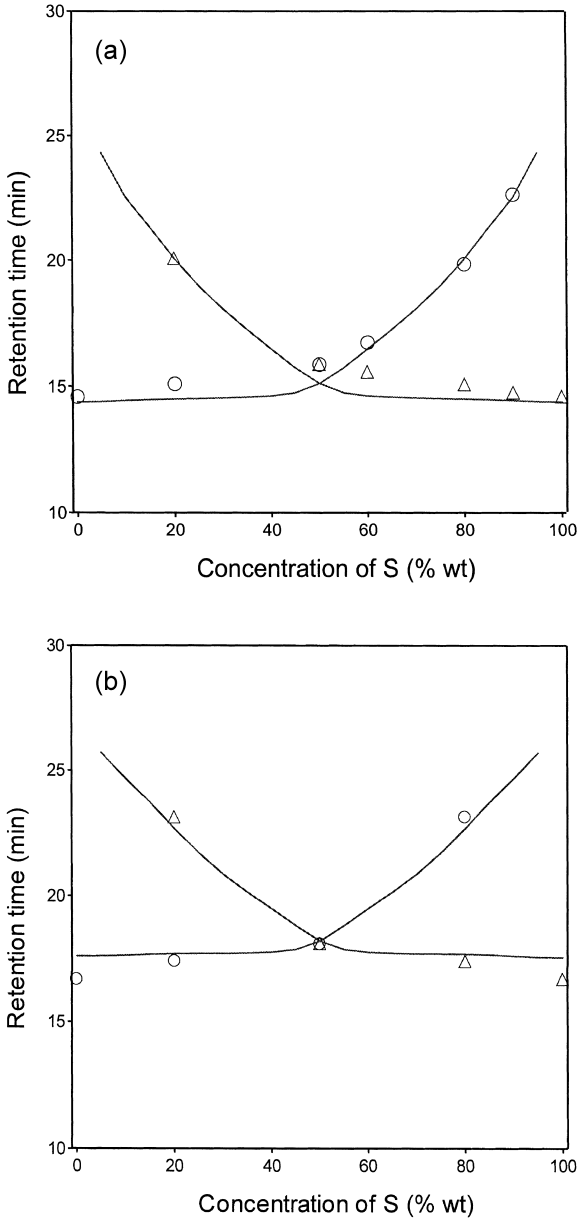

Fig. 10. Experimental (symbols) and calculated (solid line) retention times of the peak maxima of the two enantiomers for 100 μl pulses of solutions at different relative compositions. (a) 30 g/l solutions; (b) 20 g/l solutions.

equilibrium, with equilibrium constants $K_{\text{homo}} = K$ for the first two reactions (since they involve enantiomeric reactants and products), and K_{hetero} for the last one. It is assumed that there is only one independent parameter since $K_{\text{hetero}} = 2K$ on statistical grounds [10,11]. Finally, all monomeric and dimeric species are adsorbed, and follow a competitive multicomponent bi-Langmuir isotherm. Due to the symmetries exhibited by the different species the following isotherms are used:

$$\overline{m_R} = \frac{h_1 m_R}{G} + \frac{a_1 m_R}{B} \quad (7)$$

$$\overline{m_S} = \frac{h_1 m_S}{G} + \frac{a_1 m_S}{B} \quad (8)$$

$$\overline{d_{RR}} = \frac{h_2 d_{RR}}{G} + \frac{a_2 d_{RR}}{B} \quad (9)$$

$$\overline{d_{SS}} = \frac{h_2 d_{SS}}{G} + \frac{a_2 d_{SS}}{B} \quad (10)$$

$$\overline{d_{RS}} = \frac{h_3 d_{RS}}{G} + \frac{a_3 d_{RS}}{B} \quad (11)$$

where the denominators G and B are given by:

$$G = 1 + g_1(m_R + m_S) + g_2(d_{RR} + d_{SS}) + g_3 d_{RS} \quad (12)$$

$$B = 1 + b_1(m_R + m_S) + b_2(d_{RR} + d_{SS}) + b_3 d_{RS} \quad (13)$$

In the above equations m_R and m_S, and d_{RR}, d_{SS} and d_{RS} represent monomer and dimer molar concentrations, respectively. Variables with a bar refer to the adsorbed phase.

The above thermodynamic model involves five chemical species in both the fluid and the adsorbed phase. Assuming that the three chemical reactions and the adsorption of the five species are at equilibrium, then only the concentration of two species, e.g. the fluid phase concentrations m_R and m_S of the two enantiomers in monomeric form, are independent. From these values the fluid phase concentration of the three dimers can be obtained by enforcing the three chemical equilibria (1)–(3). From the fluid phase concentrations, then the five adsorbed phase concentrations are calculated using the adsorption isotherms, i.e. Eqs. (7)–(11).

5.2. Column dynamics

The above thermodynamic model has been plugged into a standard model of a chromatographic column. It is nevertheless worth elaborating a bit on the assumptions on which the model is based.

All chemical reactions in the fluid phase, as well as all adsorption phenomena are assumed to be instantaneous, i.e. at equilibrium at every time and every position along the column. This allows considering only two independent material balance equations. These are most conveniently written in terms of the overall fluid phase concentrations of the two enantiomers, i.e. r and s, which account for all the monomeric and dimeric species where they are present:

$$r = m_R + 2d_{RR} + d_{RS} \tag{14}$$

$$s = m_S + 2d_{SS} + d_{RS} \tag{15}$$

Assuming equilibrium of the dimerization reactions (1)–(3), i.e. $d_{RR} = Km_R^2$, $d_{SS} = Km_S^2$, and $d_{RS} = 2Km_Rm_S$, these can be recast as a one-to-one mapping between overall and monomeric enantiomer concentrations:

$$r = m_R + 2Km_R^2 + 2Km_Rm_S \tag{16}$$

$$s = m_S + 2Km_S^2 + 2Km_Rm_S \tag{17}$$

A similar material balance applies to the adsorbed phase:

$$\bar{r} = \overline{m_R} + 2\overline{d_{RR}} + \overline{d_{RS}} \tag{18}$$

$$\bar{s} = \overline{m_S} + 2\overline{d_{SS}} + \overline{d_{RS}} \tag{19}$$

Combining the equations above and the competitive adsorption equilibria that are based on Eqs. (7)–(11) allows expressing $\bar{r}$ and $\bar{s}$ in terms of the two independent variables m_R and m_S:

$$\bar{r} = \frac{h_1m_R + 2h_2Km_R^2 + 2h_3Km_Rm_S}{G} + \frac{a_1m_R + 2a_2Km_R^2 + 2a_3Km_Rm_S}{B} \tag{20}$$

$$\bar{s} = \frac{h_1m_S + 2h_2Km_S^2 + 2h_3Km_Rm_S}{G} + \frac{a_1m_S + 2a_2Km_S^2 + 2a_3Km_Rm_S}{B} \tag{21}$$

where the denominators G and B defined by Eqs. (12) and (13) can be recast as:

$$G = 1 + g_1(m_R + m_S) + g_2K(m_R^2 + m_S^2) + 2g_3Km_Rm_S \tag{22}$$

$$B = 1 + b_1(m_R + m_S) + b_2K(m_R^2 + m_S^2) + 2b_3Km_Rm_S \tag{23}$$

The effect of mass transfer resistance as well as that of axial dispersion associated to molecular diffusion (normally negligible in liquid chromatography) and eddy dispersion, is lumped into an apparent axial dispersion coefficient, applied for convenience directly to the overall concentrations r and s [16].

The resulting equilibrium dispersive model is constituted of the following two equations (where u is the superficial fluid velocity and ε is the overall column void fraction):

$$\varepsilon \cdot \frac{\partial r}{\partial t} + (1-\varepsilon) \cdot \frac{\partial \bar{r}}{\partial t} + u \cdot \frac{\partial r}{\partial z} = \varepsilon D_{ap} \cdot \frac{\partial^2 r}{\partial z^2} \tag{24}$$

$$\varepsilon \cdot \frac{\partial s}{\partial t} + (1-\varepsilon) \cdot \frac{\partial \bar{s}}{\partial t} + u \cdot \frac{\partial s}{\partial z} = \varepsilon D_{ap} \cdot \frac{\partial^2 s}{\partial z^2} \tag{25}$$

together with the equilibrium relationships between the adsorbed phase concentrations $\bar{r}$ and $\bar{s}$ and the fluid phase ones r and s. These relationships are implicitly defined by Eqs. (16), (17), (20), and (21). In fact Eqs. (16) and (17) can be explicitly inverted yielding:

$$m_R = \frac{2r}{1 + \sqrt{1 + 8K(r+s)}} \tag{26}$$

$$m_S = \frac{2s}{1 + \sqrt{1 + 8K(r+s)}} \tag{27}$$

Substituting the last equations into Eqs. (20) and (21), and the resulting equations into the partial differential Eqs. (24) and (25) yields a system of PDEs in the unknowns r and s only. Once this is solved and r and s are obtained as functions of time and space, Eqs. (26) and (27) are used once more to calculate the concentrations m_R and m_S, through which all the other concentration values can be calculated. More details about this variable transformation are provided in Appendix A.

5.3. Parameter estimation

The mathematical model developed above involves a number of parameters that have been estimated either through direct experimental measurements or through fitting of the experimental chromatograms. To the former group belong the dimerization equilibrium constant discussed above, and the overall column void fraction measured using an inert tracer; the obtained values are $K = 2.4$ l/mol, and $\varepsilon = 0.73$. The superficial flow velocity was in all experiments $u = 7.96$ cm/min, i.e. corresponding to a flow-rate of 1 ml/min, which is typical in analytical chromatography. Actually, the axial dispersion coefficient has not been evaluated as such since the numerical solution of the equilibrium axial dispersive model has been obtained by using a finite difference scheme where the discretization is set so that the corresponding numerical dispersion plays the role of the apparent axial dispersion [16]. Therefore, for the sake of simplicity this approach has been adopted in all the following calculations, by using a space discretisation of the column yielding up to 5000 theoretical stages, which can be considered a realistic value for analytical columns.

5.3.1. Adsorption isotherms

The remaining parameters of the model are those of the adsorption isotherms and these have been estimated through the approach described in the following. It is worth noting that the objective was to achieve a good description of the system in terms of retention times, i.e. resolution of the two peaks that are experimentally observed, in order to validate the reliability of the physico-chemical model described above. The agreement between model calculations and experimental results in terms of details of the elution profiles was not considered as a primary objective, and has been checked only for the sake of completeness.

The adsorption isotherm parameters in Eqs. (7)–(13) are twelve: h_1, g_1, a_1, b_1, h_2, g_2, a_2, b_2, h_3, g_3, a_3, and b_3. However, not all of them are independent. In fact, the physical picture behind the bi-Langmuir isotherm is that of adsorption on two types of adsorption sites; the ratios $N_i = h_i/g_i$ and $Q_i = a_i/b_i$ $(i = 1, \ldots, 3)$ define the corresponding molar loading capacities for the monomers $(i = 1)$, the homochiral dimers $(i = 2)$, and the heterochiral dimers $(i = 3)$. Therefore, since it is physically sound to require that the molar loading capacities of monomers is double that of dimers, the following constraints must be fulfilled:

$$g_i = 2g_1 h_i/h_1 \quad (i = 2, 3) \tag{28}$$

$$b_i = 2b_1 a_i/b_1 \quad (i = 2, 3) \tag{29}$$

thus reducing the number of independent parameters to eight. This number is rather large, in principle. However, one should keep in mind that a system with adsorbates following three different adsorption isotherms is considered, and that the adsorption equilibria of this type of components are commonly found to be so complex as to require a bi-Langmuir isotherm, which requires four parameters for each species, to be described. On the other hand, as shown in the following, we have designed chromatographic experiments that allow to estimate these parameters at least partially independently.

5.3.2. Monomers and homochiral dimers

The chromatographic behaviour of pulses constituted of a single enantiomer and illustrated in Figs. 1 and 2 depends on the adsorption isotherm of monomers and homochiral dimers only, i.e. on the six parameters h_1, g_1, a_1, b_1, h_2, and a_2. Through Eqs. (28) and (29), g_2, and b_2 are calculated from these six independent parameters. These have been estimated by fitting the retention time measurements reported in Fig. 2. In this case the retention times have been calculated using a simple local equilibrium model constituted of a single first order partial differential equation, i.e. either Eq. (24) or Eq. (25), without the axial dispersion term; the calculation procedure is reported in detail in Appendix B. The calculated results obtained using the best-fit parameters reported in the caption of Fig. 2 and plotted as a solid line exhibit a rather good agreement with the experimental measurements both at small and large injected amounts.

A few remarks about the fitting procedure and the obtained parameters are necessary. The loading capacity associated with the first term in the bi-Langmuir isotherms, i.e. $N_1 = h_1/g_1 = 0.43$ m*M*, is about 200 times smaller than the loading capacity associated with the second type of sites, i.e. $Q_1 = a_1/$

$b_1 = 76$ mM. Thus the sites of the first type are highly energetic, highly selective (as it will be shown later), and have a rather small adsorption capacity. The behaviour of pulse chromatograms at small amounts injected (see insert of Fig. 2) is controlled by the parameters h_1, g_1, and h_2, and is rather insensitive to parameters a_1, b_1, and a_2. On the contrary, the sites of the second type exhibit lower energy of interaction, but have a much larger capacity, thus controlling the adsorption behaviour at large amounts injected through the parameters a_1, b_1, and a_2. This allows to determine the two sets of three parameters almost independently. However, a major difficulty arises when trying to discriminate between the adsorption behaviour of the monomers and that of the homochiral dimers. As a matter of fact it can be observed that changing the ratios h_2/h_1 and a_2/a_1 in the range 0.001 to 20 yields no significant difference in the calculated retention time values in the whole range of amounts injected investigated. This means that the selectivity of the stationary phase between homochiral dimers and monomers cannot be determined from our chromatographic measurements. Therefore, we have decided to set it equal to one, i.e. we have enforced the conditions $h_2 = h_1$ and $a_2 = a_1$.

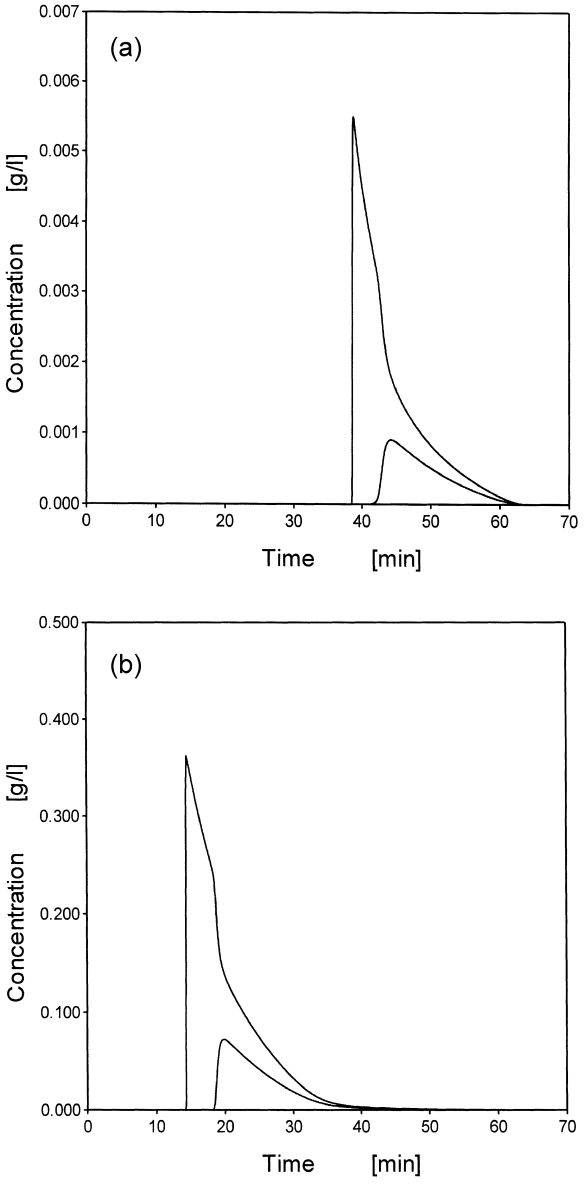

Fig. 11. Calculated elution profiles of a 80:20 solution of $S(-)$- and $R(+)$-1-1′-bi-2-naphthol enantiomers. (a) 20 μl pulse at 2 g/l total concentration; (b) 100 μl pulse at 30 g/l total concentration.

Thus concluding, only two pairs of independent parameters have been used to fit the data in Fig. 2, which control the low and high concentration behaviour, respectively. The best-fit values obtained are: $h_1 = h_2 = 32$, $a_1 = a_2 = 38$, $g_1 = g_2/2 = 74$ l/mmol, and $b_1 = b_2/2 = 0.5$ l/mmol.

5.3.3. Heterochiral dimers

The formation and the adsorption of heterochiral dimers control the enantiomeric enrichment achieved in pulse chromatograms of non-racemic mixtures. Due to the assumptions leading to Eqs. (28) and (29), only two independent parameters, i.e. h_3 and a_3, control the behaviour of the model when simulating such chromatograms. These have been estimated by fitting with the equilibrium dispersive model of Eqs. (24) and (25) the retention time data reported in Fig. 10a and 10b, as well as those of low concentration experiments such as the one in Fig. 3. A rather good qualitative and quantitative agreement between calculated retention times (solid lines) and experimental measurements (symbols) is obtained as shown in Fig. 10.

This is further confirmed when the calculated elution profiles of the two enantiomers are compared with the experimental chromatograms. For the sake of brevity the results of only two simulations are reported, namely those in Fig. 11a at low con-

centration and in Fig. 11b at high concentration that compare with Fig. 3 and Fig. 6, respectively. Also in the case of concentration profiles, most of the experimentally observed features are properly described by the model, particularly the achievement of 100% e.e. in the first eluting fraction, and the slow decay of e.e. in the tail of the second fraction. It is worth noting that the breakthrough times of the adsorption fronts of the two enantiomers as well as the concentrations at the peak maxima compare well with the measured values.

These rather satisfactory results have been achieved using large values of the two free parameters, namely with $h_3 = 2000h_1 = 64\,000$, and $a_3 = 330$, and therefore with $g_3 = 296 \times 10^3$ l/mmol, and $b_3 = 8.68$ l/mmol according to Eqs. (28) and (29). These somehow surprisingly high values of selectivity are necessary to describe the large separation of the two peaks, which is observed at both high and low concentration. This is the case, since the extent of dimerization achieved with the dimerization equilibrium constant that has been independently measured is relatively small. Therefore, the obtained selectivity values reflect indeed the features of this system. In addition, it is worth highlighting that for the same system also Nicoud and coworkers, who were using a similar model, used a selectivity between heterochiral and homochiral dimers of more than 300 to describe chromatograms where a resolution between the two enantiomers in non-racemic pulses significantly worse than in our experiments was observed [9].

6. Conclusions

In this work two significant results are obtained. On the one hand, it has been shown that a non-racemic pulse of the two enantiomers can be split into two fractions where the first one contains only the excess enantiomer with a 100% e.e., whereas the second is constituted of an almost racemic mixture of the two enantiomers. The resolution is so good and the amount of pure enantiomer recovered is so large that a preparative application of this phenomenon could be envisaged. This confirms and further improves previous results reported in the literature about the same system and different ones.

On the other hand, a mathematical model has been developed, which is able to describe qualitatively and quantitatively all the observed phenomena and effects. This is based on accounting for the occurrence of dimerization through chemical equilibria, whose equilibrium constant has been measured independently. Moreover, the adsorption of the enantiomers in monomeric and dimeric form is described through competitive bi-Langmuir isotherms. Some physically reasonable constraints on the loading capacity of monomers and dimers on the two types of bi-Langmuir sites have been enforced, thus reducing the overall number of adsorption isotherm parameters. These have been estimated by fitting the retention times observed in a large number of pulse chromatograms. It was found that the experimental data do not allow for the determination of the selectivity between monomers and homochiral dimers, but indicate clearly that the selectivity between heterochiral and homochiral dimers is extremely large.

The model should be viewed as a valuable tool for describing the system within the rather large range of concentrations explored. We believe that this could significantly help to explore the possibility of applying achiral chromatography in the preparative purification of non-racemic mixtures of enantiomers. However, extrapolation of the model to larger concentrations should be done with caution. This is very true in this particular case, due to the large selectivity exhibited by the system, for which no physicochemical explanation has been found so far. It might be that our description of the adsorption behaviour of the system is oversimplified, and that a more sophisticated adsorption model should be used, possibly including explicitly the effect of the presence of the solvent.

7. Nomenclature

a_1, a_2, a_3	bi-Langmuir isotherm parameters (–)
A	UV absorbance (V)
b_1, b_2, b_3	bi-Langmuir isotherm parameters (l/mmol)
B	denominator in the bi-Langmuir isotherm (–)
c	overall fluid concentration, $c = r + s$ (M)

d_{ii}	fluid concentration of dimers (ii = *RR*,*SS*,*RS*) (M)
$\overline{d_{ii}}$	adsorbed concentration of dimers (ii = *RR*, *SS*, *RS*) (M)
D	UV absorbance coefficient for homochiral dimers (V l/mol)
D_{ap}	effective axial dispersion (cm^2/s)
e.e.	enantiomeric excess (–)
g_1, g_2, g_3	bi-Langmuir isotherm parameters (l/mmol)
G	denominator in the bi-Langmuir isotherm (–)
h_1, h_2, h_3	bi-Langmuir isotherm parameters (–)
J	determinant of the jacobian, defined by Eq. (A.11) (–)
K	homochiral dimerization equilibrium constant (l/mol)
K_r	dimerization equilibrium constant (r = *homo*, *hetero*) (l/mol)
m	overall fluid concentration of enantiomers in monomeric form, $m = m_R + m_S$ (M)
m_i	fluid concentration of enantiomers in monomeric form ($i = R, S$) (M)
$\overline{m_i}$	adsorbed concentration of enantiomers in monomeric form ($i = R, S$) (M)
M	UV absorbance coefficient for enantiomers in monomeric form (V l/mol)
N_i	loading capacity in the bi-Langmuir isotherm, $N_i = h_i/g_i$ (mol/l)
N_{inj}	injected amount in a chromatographic pulse (mol)
P	polarimeter signal (V)
Q	fluid flow-rate, $N_i = h_i/g_i$ (l/s)
Q_i	loading capacity in the bi-Langmuir isotherm, $Q_i = a_i/b_i$ (M)
r	overall fluid concentration of the **R** enantiomer (M)
$\bar{r}$	overall adsorbed concentration of the **R** enantiomer (M)
s	overall fluid concentration of the **S** enantiomer (M)
$\bar{s}$	overall adsorbed concentration of the **S** enantiomer (M)
t	time (s)
u	superficial fluid velocity (cm/s)
V	column volume (l)
z	axial coordinate (cm)

Greek letters

δ	polarimeter coefficient for enantiomers in monomeric form (V l/mol)
μ	polarimeter coefficient for homochiral dimers (V l/mol)

Subscripts and superscripts

homo	homochiral dimerization
hetero	heterochiral dimerization
p	peak maximum
R	**R** enantiomer
RR	**RR** dimer
RS	**RS**dimer
S	**S** enantiomer
SS	**SS** dimer

Acknowledgements

R.B. wishes to express his gratitude to the late Professor Marina Attinà for her continuous encouragement and support in this project. M.M. wishes to thank Professor A.S. Dreiding for stimulating his interest in the achiral chromatography of enantiomers.

Appendix A

This appendix describes how to treat the two partial derivatives $\partial\bar{r}/\partial t$ and $\partial\bar{s}/\partial t$ in Eqs. (24) and (25). These can be recast as:

$$\frac{\partial\bar{r}}{\partial t} = \frac{\partial\bar{r}}{\partial r}\cdot\frac{\partial r}{\partial t} + \frac{\partial\bar{r}}{\partial s}\cdot\frac{\partial s}{\partial t} \tag{A.1}$$

$$\frac{\partial\bar{s}}{\partial t} = \frac{\partial\bar{s}}{\partial r}\cdot\frac{\partial r}{\partial t} + \frac{\partial\bar{s}}{\partial s}\cdot\frac{\partial s}{\partial t} \tag{A.2}$$

The needed partial derivatives can be written as follows:

$$\frac{\partial\bar{r}}{\partial r} = \frac{\partial\bar{r}}{\partial m_R}\cdot\frac{\partial m_R}{\partial r} + \frac{\partial\bar{r}}{\partial m_S}\cdot\frac{\partial m_S}{\partial r} \tag{A.3}$$

$$\frac{\partial\bar{r}}{\partial s} = \frac{\partial\bar{r}}{\partial m_R}\cdot\frac{\partial m_R}{\partial s} + \frac{\partial\bar{r}}{\partial m_S}\cdot\frac{\partial m_S}{\partial s} \tag{A.4}$$

$$\frac{\partial\bar{s}}{\partial r} = \frac{\partial\bar{s}}{\partial m_R}\cdot\frac{\partial m_R}{\partial r} + \frac{\partial\bar{s}}{\partial m_S}\cdot\frac{\partial m_S}{\partial r} \tag{A.5}$$

$$\frac{\partial \bar{s}}{\partial s} = \frac{\partial \bar{s}}{\partial m_R} \cdot \frac{\partial m_R}{\partial s} + \frac{\partial \bar{s}}{\partial m_S} \cdot \frac{\partial m_S}{\partial s} \tag{A.6}$$

On the one hand, the four partial derivatives $\partial \bar{r}/\partial m_R$, $\partial \bar{r}/\partial m_S$, $\partial \bar{s}/\partial m_R$, and $\partial \bar{s}/\partial m_S$ are given by straightforward though lengthy relationships obtained by differentiating Eqs. (20) and (21). On the other hand, the four partial derivatives $\partial m_R/\partial r$, $\partial m_R/\partial s$, $\partial m_S/\partial r$, and $\partial m_S/\partial s$ are:

$$\frac{\partial m_R}{\partial r} = \frac{1}{J} \cdot \frac{\partial s}{\partial m_S} = \frac{1 + 4Km_S + 2Km_R}{J} \tag{A.7}$$

$$\frac{\partial m_R}{\partial s} = -\frac{1}{J} \cdot \frac{\partial r}{\partial m_S} = -\frac{2Km_R}{J} \tag{A.8}$$

$$\frac{\partial m_S}{\partial r} = -\frac{1}{J} \cdot \frac{\partial s}{\partial m_R} = -\frac{2Km_S}{J} \tag{A.9}$$

$$\frac{\partial m_S}{\partial s} = \frac{1}{J} \cdot \frac{\partial r}{\partial m_R} = \frac{1 + 4Km_R + 2Km_S}{J} \tag{A.10}$$

where

$$\begin{aligned} J &= \frac{\partial r}{\partial m_R} \cdot \frac{\partial s}{\partial m_S} - \frac{\partial s}{\partial m_R} \cdot \frac{\partial r}{\partial m_S} \\ &= (1 + 4Km_R + 2Km_S)(1 + 4Km_S + 2Km_R) \\ &\quad - 2K^2 m_R m_S \end{aligned} \tag{A.11}$$

is the determinant of the jacobian of the transformation $(m_R, m_S) \mapsto (r, s)$ defined by Eqs. (16) and (17).

Appendix B

This appendix deals with the pulse chromatography of a single enantiomer, say enantiomer **R**, under overload conditions. In the frame of equilibrium theory, i.e. neglecting the second order derivatives in Eqs. (24) and (25), it is rather straightforward to derive an explicit relationship for the retention time of the peak maximum. This is obtained by enforcing the constraint that the whole amount of the species injected, i.e. N_{inj}, must be equal to the amount collected at the outlet, which is proportional to the integral of the peak profile at the column outlet:

$$N_{\text{inj}} = Q \int_0^\infty r \, \mathrm{d}t \tag{B.1}$$

where Q is the volume flow-rate, and the concentration r and the corresponding elution time are related through the classical equilibrium theory equation:

$$t = \frac{V}{Q} \cdot \left(\varepsilon + (1 - \varepsilon) \cdot \frac{\mathrm{d}\bar{r}}{\mathrm{d}r} \right) \tag{B.2}$$

Differentiating the last equation and substituting it into Eq. (B.1), and then integrating by parts between the concentration corresponding to the peak maximum $r = r_p$ and $r = 0$ yields:

$$N_{\text{inj}} = V(1 - \varepsilon) \cdot \left(\bar{r} - r \cdot \frac{\mathrm{d}\bar{r}}{\mathrm{d}r} \right)_{r = r_p} \tag{B.3}$$

where the whole term between brackets is evaluated at the concentration r_p. The last relationship establishes a one-to-one mapping between the amount injected N_{inj} and the concentration at the peak maximum r_p. Through Eq. (B.2) evaluated at r_p the corresponding elution time of the peak maximum t_p is obtained, thus establishing the relationship $N_{\text{inj}} \mapsto t_p$, which is plotted in Fig. 2 (solid line) and can be compared with the experimental results (symbols).

The terms related to the adsorbed amount $\bar{r}$ and its derivative in the equations above can be obtained from the following relationships, which are just special cases of Eqs. (20), (A.3), (A.7), and (A.11), where $m_S = s = 0$:

$$\bar{r} = \frac{h_1 m_R + 2h_2 K m_R^2}{1 + g_1 m_R + g_2 K m_R^2} + \frac{a_1 m_R + 2a_2 K m_R^2}{1 + b_1 m_R + b_2 K m_R^2} \tag{B.4}$$

$$\frac{\mathrm{d}\bar{r}}{\mathrm{d}r} = \frac{\mathrm{d}\bar{r}}{\mathrm{d}m_R} \cdot \frac{\mathrm{d}m_R}{\mathrm{d}r} = \frac{1}{(1 + 4Km_R)} \cdot \frac{\mathrm{d}\bar{r}}{\mathrm{d}m_R} \tag{B.5}$$

$$\begin{aligned} \frac{\mathrm{d}\bar{r}}{\mathrm{d}m_R} = {} & \frac{h_1 + 4h_2 K m_R + K m_R^2 (2h_2 g_1 - h_1 g_2)}{(1 + g_1 m_R + g_2 K m_R^2)^2} \\ & + \frac{a_1 + 4a_2 K m_R + K m_R^2 (2a_2 b_1 - a_1 b_2)}{(1 + b_1 m_R + b_2 K m_R^2)^2} \end{aligned} \tag{B.6}$$

References

[1] M. Juza, M. Mazzotti, M. Morbidelli, Trends Biotechnol. 18 (2000) 108.
[2] K.C. Cundy, P.A. Crooks, J. Chromatogr. 281 (1983) 17.
[3] R. Charles, E. Gil-Av, J. Chromatogr. 298 (1984) 516.
[4] W.-L. Tsai, K. Hermann, E. Hug, B. Rohde, A.S. Dreiding, Helv. Chim. Acta 68 (1985) 2238.
[5] A. Dobashi, Y. Motoyama, K. Kinoshita, S. Hara, N. Fukasaku, Anal. Chem. 59 (1987) 2209.
[6] R. Matusch, C. Coors, Angew. Chem., Int. Ed. Engl. 28 (1989) 626.
[7] P. Diter, S. Taudien, O. Samuel, H.B. Kagan, J. Org. Chem. Eng. 59 (1994) 370.
[8] R. Stephani, V. Cesare, J. Chromatogr. A 813 (1998) 179.
[9] R.-M. Nicoud, J.-N. Jaubert, I. Rupprecht, J. Kinkel, Chirality 8 (1996) 234.
[10] R. Baciocchi, G. Zenoni, M. Valentini, M. Mazzotti, M. Morbidell, J. Phys. Chem. A (2001) submitted for publication.
[11] M. Jung, V. Schrurig, J. Chromatogr. 605 (1992) 161.
[12] A. Kurganov, Chromatographia 43 (1996) 17.
[13] E. Gil-Av, V. Schurig, J. Chromatogr. A 666 (1994) 519.
[14] G. Zenoni, M. Pedeferri, M. Mazzotti, M. Morbidelli, J. Chromatogr. A 888 (2000) 73.
[15] E.L. Eliel, S.H. Wilen, L.N. Mander, Stereochemistry of Organic Compounds, Wiley-Interscience, 1993.
[16] C. Migliorini, A. Gentilini, M. Mazzotti, M. Morbidelli, Ind. Eng. Chem. Res. 38 (1999) 2400.